

Kinetic Analysis of Barley Chitinase¹

Thomas Hollis,* Yuji Honda,† Tamo Fukamizo,† Edward Marcotte,*
Philip J. Day,* and Jon D. Robertus*,²

*Department of Chemistry and Biochemistry, University of Texas, Austin Texas 78712; and

†Department of Food and Nutrition, 3327-204 Nakamachi, Nara 631, Japan

Received March 10, 1997, and in revised form May 30, 1997

The endochitinase from barley is the archetypal enzyme for a large class of plant-derived antifungal chitinases. The X-ray structure was solved previously in our laboratory and a mechanism of action proposed based on structural considerations. In this manuscript we report the use of a defined soluble substrate, 4-methylumbelliferyl β -N,N',N'-triacetylchitotrioside, to characterize kinetic parameters of the enzyme. The pH profile shows that activity is controlled by a base with a pK_a of 3.9 (Glu 89) and an acid with a pK_a of 6.9 (Glu 67). The K_m using the synthetic substrate is 33 μM , and the k_{cat} is 0.33 min^{-1} , while the K_m for (GlcNAc)₄ is 3 μM and k_{cat} is 35 min^{-1} . Binding constants were measured for β -linked oligomers of N-acetylglucosamine. The monomer does not bind and dissociation constants for the dimer, trimer, and tetramer are 43, 19, and 6 μM , respectively. Analysis of kinetic and dissociation constants proves the mechanism of barley chitinase is consistent with a Bi-Bi kinetic model for hydrolysis, with (GlcNAc)₄ and water as substrates and (GlcNAc)₂ as products. Substrate cleavage patterns show that (GlcNAc)₆ is cleaved in half to (GlcNAc)₃ as well as into (GlcNAc)₄ and (GlcNAc)₂ with almost equal efficiency. NMR analysis of cleavage products confirms that the enzyme proceeds with anomeric inversion of products.

© 1997 Academic Press

Key Words: glycohydrolase; enzyme mechanism; chitin binding.

Plants produce a variety of pathogenesis-related proteins³ in response to stress or infection. The largest

group of these proteins is the lytic enzymes which is composed primarily of β , 1-3 glucanases and chitinases. In their role as defense proteins, these enzymes limit fungal growth by hydrolyzing (1-3) β glucan and chitin, a β , 1-4-linked polymer of N-acetylglucosamine (GlcNAc)³, the major structural polysaccharides of fungal cell walls. The actions of these two enzymes as antifungal agents either alone (1-4) or acting synergistically (5) has been well documented. Four classes of plant chitinases have been proposed based on amino acid sequence (6, 7). Classes I, II, and IV have homologous catalytic domains, but classes I and IV also possess a N-terminal cysteine-rich domain homologous to wheat germ agglutinin. Class III chitinases show little sequence similarity to the enzymes in classes I, II, or IV and are more prevalent in fungi and bacteria than in higher plants. They also seem to possess reduced antifungal activity compared to the class II enzymes, presumably because they possess a different substrate specificity (1).

Barley endochitinase, a class II chitinase, is a 26-kDa monomeric enzyme. It has moderate to high sequence identity with other class II plant chitinases from tobacco, potato, arabidopsis, and rice (8). The X-ray structure of barley chitinase has been solved (9) and refined to 1.8 Å resolution (8). The structure shows a globular protein with high α -helical content and an elongated cleft running the length of the protein, presumably for substrate binding and catalysis. Hypothetical substrate binding models with the structure suggest that there are at least six sugar-binding sites labeled A through F from the nonreducing end (8). Residues Glu 67 and Glu 89 are thought to be involved in hydrolytic catalysis, cleaving the substrate between sites D and E (10). The putative mechanism involves protonation of the glycosidic bond at the C4 oxygen of the leaving E sugar, by Glu 67. At the same time, Glu 89 may act as a base to activate a water molecule which attacks the C1 position of the D sugar on the α side. This mechanism, suggesting that the barley chitinase mechanism

¹ This work was supported by grants GM 30048 and GM35989 from the National Institutes of Health and by grants from the Foundation for Research and the Welch Foundation.

² To whom correspondence should be addressed. E-mail: jrobertus@mail.utexas.edu.

³ Abbreviations used: GlcNAc, N-acetylglucosamine; (GlcNAc)₃ UMB, 4-methylumbelliferyl β -N,N',N'-triacetylchitotrioside.

proceeds with inversion of product, is proven chemically in this paper.

It has also been shown that barley chitinase is the archetypal enzyme of a superfamily of glycohydrolases which include the plant chitinases, bacterial chitosanases, and lysozymes from hen, goose, and T4 phage (11). Despite exhibiting no significant amino acid sequence similarities, these proteins were shown to be structurally related, containing an ancient core domain which binds substrates. Although bacterial and eucaryotic glycohydrolases have differing N- and C-terminal domains, the common core unifies classes 19, 22, 23, 24, and 46 in the sequence-based classification scheme proposed by Henrissat (12).

Although the plant chitinases have been analyzed qualitatively regarding their antifungal activity, very little is known about their enzyme kinetics. Partly this is due to the fact that chitin is an insoluble polymer and therefore an inappropriate substrate for initial rate kinetics. Koga *et al.* (13) analyzed the hydrolysis of β -linked oligo (GlcNAc) substrates for the chitinase from yam, a homologue of the barley enzyme. They showed, for example, that (GlcNAc)₆ was primarily cleaved into (GlcNAc)₄ and (GlcNAc)₂, that (GlcNAc)₄ was cleaved in half, and that (GlcNAc)₂ could not be hydrolyzed. The K_m for (GlcNAc)₆ was roughly 10 μM , and the turnover number, k_{cat} , was $\sim 25 \text{ min}^{-1}$. In this paper we report the kinetic and binding parameters for barley endochitinase, the only member of this family for which an X-ray structure exists. In addition to (GlcNAc)₄, a soluble artificial substrate is used to observe initial rates, and binding constants for small oligomers of natural substrates are observed by fluorescence.

MATERIALS AND METHODS

Chitinase was purified from barley by the methods of Leah *et al.* (4). The kinetic assays were performed using both 4-methylumbelliferyl β -N,N',N'-triacetylchitotrioside ((GlcNAc)₃UMB) and (GlcNAc)₄ (Sigma). (GlcNAc)₃UMB was dissolved in 0.1 M sodium phosphate buffer, pH 6.0. Then, 95 μl of substrate solutions, ranging in concentration from 0 to 0.25 mM, were mixed with 5 μl of enzyme (0.27 mg/ml) and incubated at 30°C. for 1.5, 2.5, and 3.5 h. The reactions were stopped by adding 2.9 ml of 0.5 M glycine, pH 10.5. Release of free methylumbelliferon was measured by fluorescence spectrophotometry, using an SLM 8000 fluorescence spectrophotometer, exciting at 360 nm, and measuring emission at 450 nm. A standard curve of free methylumbelliferon was constructed and shown to be linear over the range of product measured; this allowed the conversion of fluorescence counts to nmoles of methylumbelliferon released per hour.

For the kinetics using (GlcNAc)₄ a modified reducing sugar assay was used (14). Reactions (300 μl) containing substrate ranging from 0 to 0.25 mM in 0.1 M sodium phosphate buffer, pH 6.0, and 5.2 μg chitinase were incubated for 2 h at 30°C. Reactions were stopped by adding 700 μl of water and 1 ml of solution A (0.35 M sodium carbonate, 0.2 M glycine, and 3.0 mM copper sulfate) and solution B (0.12% neocuproine) to each. The reactions were then heated to 95°C for exactly 9.0 min. Formation of reducing sugars was measured by

reading the absorption of a 1:5 dilution at 450 nm. A standard curve using GlcNAc was constructed as above, and shown to be linear over the range of product measured, allowing the conversion of absorption units to nmoles reducing ends produced per hour.

Initial rate velocities were fit to the hyperbolic rate equation using the program SigmaPlot (Jandel Scientific) to determine K_m and V_{max} values. These were also computed from double reciprocal and Eadie-Hofstee plots; all calculations produced similar values for each substrate.

Binding constants for GlcNAc, (GlcNAc)₂, (GlcNAc)₃, (GlcNAc)₄, and (GlcNAc)₃UMB (Sigma), the only defined substrates which are commercially available, were determined by measuring the change in intrinsic chitinase (1 μM protein) fluorescence while titrating with ligand at pH 7. Measurements were made by exciting at 290 nm and measuring fluorescence emission at 340 nm for (GlcNAc)_n and 290 and 325 nm for (GlcNAc)₃UMB. As a control, ligands were also titrated into free tryptophan (6 μM), which showed no change in fluorescence. The final titration of ligand did not exceed 5% of the starting volume. Complete titration and fluorescent measurements for each oligosaccharide were done within a 5-min time span to make hydrolysis of sugars a negligible factor. The results were plotted as [1-(fluorescence with ligand (F_1)/no ligand (F_0))] vs ligand concentration.

pH-dependent kinetic studies were done in 0.1 M citrate, acetate, phosphate, and Tris buffers. Reactions were run at each pH for 1, 2, and 3 h. Data were fit to a line using Sigma plot; slopes were normalized against the largest value and plotted against pH.

Anomer analysis of the product was carried out through NMR. The substrate oligosaccharide, (GlcNAc)₆, was lyophilized three times from D₂O and then dissolved in 0.6 ml of 50 mM sodium acetate-*d*₃ buffer, pH 4.3. The purified chitinase solution was concentrated and dialyzed against the sodium acetate-*d*₃ buffer using a Centricon concentrator (Amicon Co.), and 10 ml of the solution was mixed with the substrate solution in an NMR tube. The resultant concentrations of enzyme and substrate were 2.6 and 3.1 mM, respectively. The NMR tube was immediately set into an NMR probe equipped with a Jeol EX-270 spectrometer, and the enzymatic reaction was conducted in the NMR probe maintained at 25°C. After an appropriate reaction time, accumulation of the ¹H NMR spectrum was started and required 3 min. From the time-dependent profile of the spectra, the anomeric form of products was determined. As a control, the same reaction was carried out with penta-N-acetylchitopentitol, a substrate which chitinase is not able to hydrolyze. The spectrum of the reaction mixture did not change with time.

For a time course of the enzymatic reaction, the substrate oligosaccharide was dissolved in 50 mM acetate buffer, pH 5.0, and several microliters of the chitinase solution dialyzed against the same buffer was added to 0.5 ml of the substrate solution. The reaction mixture was incubated at 40°C for an appropriate period. A portion of the reaction mixture was withdrawn and mixed with the same volume of 0.5 M sodium hydroxide in order to terminate the enzymatic reaction, and the resultant solution applied to a gel-filtration column of TSK-GEL G2000PW (7.5 \times 600 mm, Tosoh). The elution was conducted with distilled water at a flow rate of 0.3 ml/min, and the substrate and the products were monitored by absorption at 220 nm. From the peak area obtained by the HPLC, oligosaccharide concentrations at each reaction time were calculated using the standard curve obtained with the authentic saccharide solution.

Determination of products from (GlcNAc)₃UMB digestion was carried out using capillary electrophoresis. Fifty microliters of reaction mixtures containing 1.5 mM substrate and 0 or 5 μg of enzyme was incubated at 30°C for 24 h. The reaction products were then separated on a Beckman P/ACE 5000 capillary electrophoresis instrument using 200 mM borate buffer with 2-s injection times and running at 7.0 V. The capillary was a 50-cm (to point of detection) non-coated standard silica capillary. Elution times were measured by monitoring absorption at 200 and 280 nm.

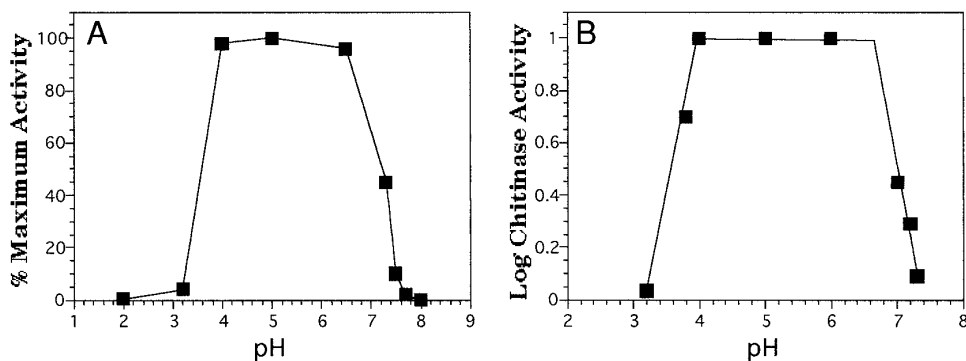


FIG. 1. The pH profile of chitinase. (A) Enzyme activity was observed under conditions of substrate saturation for the pHs indicated. Activity is expressed as a fraction of the maximum values. (B) Log of activity vs pH. Inflection points give pK_a s of 3.9 and 6.8, which are presumably for Glu 89 and Glu 67, respectively.

RESULTS

Chitinase activity against $(\text{GlcNAc})_3\text{UMB}$ was measured as a function of pH (Fig. 1A). There is no measurable activity below pH 3.2, at which point there is a dramatic increase in activity as the pH rises to 4. The enzyme remains fully active until pH 7, followed by a precipitous drop in activity above pH 8. Figure 1B shows a plot of the log of activity vs pH. The ascending limb has a slope of 1 with a $pK_a \sim 3.9$; the descending limb has a slope of 1 and $pK_a \sim 6.8$.

The results of the kinetic analysis of barley chitinase, using $(\text{GlcNAc})_3\text{UMB}$ substrate concentrations from 1 mM to 250 μM , are represented in Fig. 2A. The hyperbolic plot of the data shows that the enzyme has a K_m of 33 μM , a V_{\max} of 12 nmol/min/mg enzyme, and a k_{cat} of 0.36 min^{-1} . From this, the catalytic efficiency, k_{cat}/K_m , is calculated to be $1.7 \times 10^2 \text{ M}^{-1} \text{ s}^{-1}$. Figure 2B shows the results of the kinetic assay using $(\text{GlcNAc})_4$. With this substrate, the enzyme has a K_m of 3 μM , a V_{\max} of 1.2 $\mu\text{mol}/\text{min}/\text{mg}$ enzyme, a k_{cat} of 35 min^{-1} , and a k_{cat}/K_m of $1.9 \times 10^5 \text{ M}^{-1} \text{ s}^{-1}$.

Figure 3 shows the results of equilibrium binding assays with varying lengths of substrate polymer, from GlcNAc to $(\text{GlcNAc})_4$. $(\text{GlcNAc})_4$ proved to have the lowest K_d , followed by $(\text{GlcNAc})_3$ and $(\text{GlcNAc})_2$, respectively. GlcNAc alone, which is not shown in the figure, had no measurable affinity up to 500 μM . The K_d values for $(\text{GlcNAc})_4$, $(\text{GlcNAc})_3$, and $(\text{GlcNAc})_2$ are 6 ± 1 , 19 ± 2.5 , and $43 \pm 3 \mu\text{M}$, respectively. The artificial substrate $(\text{GlcNAc})_3\text{UMB}$ had a K_d of $90 \pm 7 \mu\text{M}$.

The time-dependent profile of the ^1H NMR spectrum of the chitinase reaction mixture is shown in Fig. 4A. According to the assignments reported thus far (15), the signals at 5.14 ppm ($\text{H}_{1\alpha}$) and 4.64 ppm ($\text{H}_{1\beta}$) are derived from the anomeric proton of a reducing end GlcNAc residue in α -form and in β -form, respectively. The signals at 4.5–4.6 ppm (H_1) are from the anomeric protons of the other GlcNAc residues. With progress of the reaction time, the peak area of the signals of H_1 decreased, and those of $\text{H}_{1\alpha}$ and $\text{H}_{1\beta}$ increased. $\text{H}_{1\alpha}$ increased rapidly in the early stages of the reaction, while the increment of $\text{H}_{1\beta}$ was quite gradual. The

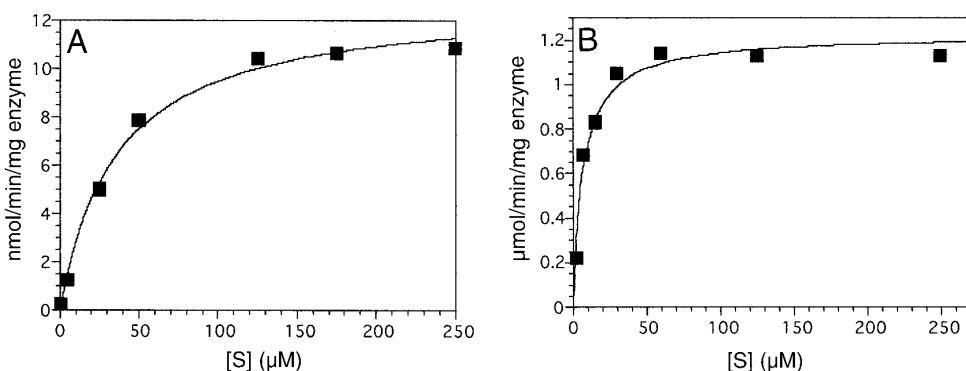


FIG. 2. Initial rate activity of barley chitinase. A direct plot of velocity data as a function of substrate concentrations shows hyperbolic kinetics. (A) $V_{\max} = 12 \text{ nmol}/\text{min}/\text{mg}$ enzyme and $K_m = 33 \mu\text{M}$ for $(\text{GlcNAc})_3\text{UMB}$ hydrolysis. (B) $V_{\max} = 1.2 \mu\text{mol}/\text{min}/\text{mg}$ and $K_m = 3 \mu\text{M}$ for $(\text{GlcNAc})_4$.

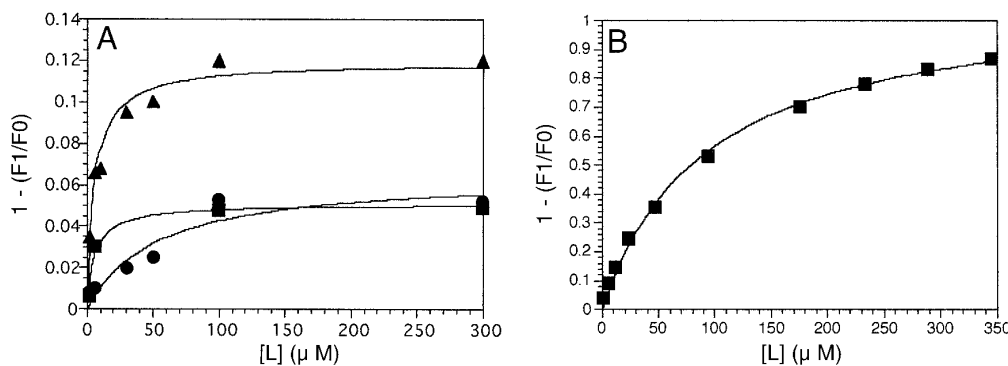


FIG. 3. Chitinase binding of oligomers. F_1/F_0 = fluorescence of chitinase with ligand/no ligand. (A) Triangles, $(\text{GlcNAc})_4$ ($K_d = 6 \mu M$); squares, $(\text{GlcNAc})_3$ ($K_d = 19 \mu M$); circles, $(\text{GlcNAc})_2$ ($K_d = 43 \mu M$). (B) $(\text{GlcNAc})_3\text{UMB}$ ($K_d = 90 \mu M$).

time courses of relative peak areas of individual signals are also shown in Fig. 4B. From these figures, it was found that the chitinase produces only the α -form, which is then transformed to the β -form by mutarotation. Chitinase from *Hordeum vulgare* L. seeds is therefore an inverting enzyme.

To obtain information on subsite structure and characteristics of the enzymatic reaction, it is essential to analyze experimental time courses of oligosaccharide degradation and product formation. As shown in Fig. 5A, $(\text{GlcNAc})_6$ was hydrolyzed to $(\text{GlcNAc})_3 + (\text{GlcNAc})_3$ and $(\text{GlcNAc})_2 + (\text{GlcNAc})_4$; the efficiencies of the two cleavages were almost identical. Equal amounts of $(\text{GlcNAc})_3$ and $(\text{GlcNAc})_2$ were produced from $(\text{GlcNAc})_5$, and only $(\text{GlcNAc})_2$ was detectable from $(\text{GlcNAc})_4$ (Figs. 5B and 5C). Figure 6 shows the results of $(\text{GlcNAc})_3\text{UMB}$ hydrolysis with barley chitinase. As expected from the hydrolysis of natural substrate, the major product is cleavage into $(\text{GlcNAc})_2$ and (GlcNAc) umbelliferone. Fluorescence arises only from free umbelliferone, so it is clear that some of the substrate is hydrolyzed between $(\text{GlcNAc})_3$ and the umbelliferyl group. We have not been able to quantitate the exact amount of this cleavage relative to the major products, but it is clear that over 90% of the $(\text{GlcNAc})_3\text{UMB}$ cleavage does not produce fluorescent umbelliferone.

DISCUSSION

We have proposed a mechanism of action for chitinase, based largely on the X-ray structure and modeling of substrate binding (8, 11). Some elements of this hypothesis, appropriate to the fluorescent substrate used in this study, are shown in Fig. 7. The cleavage site lies between sugar binding sites D and E on the

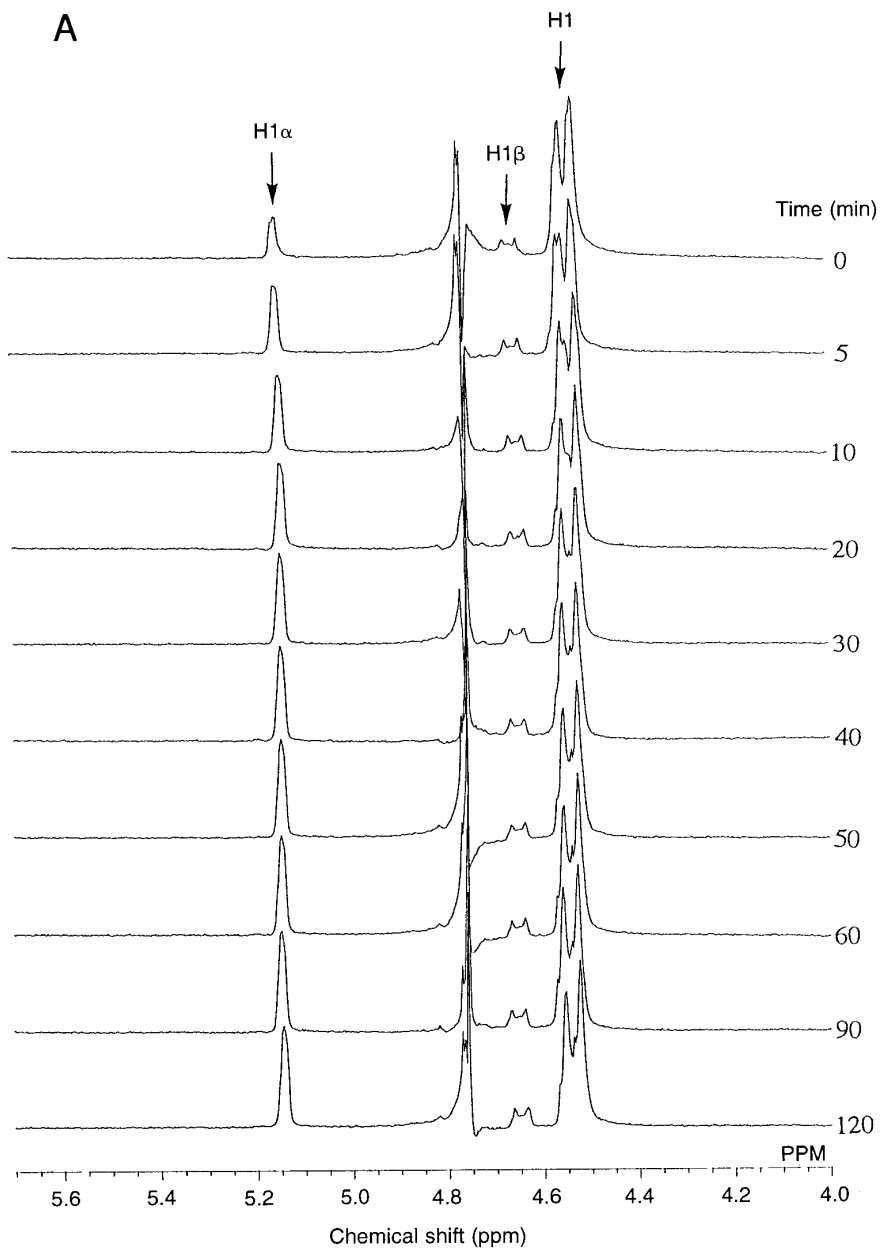
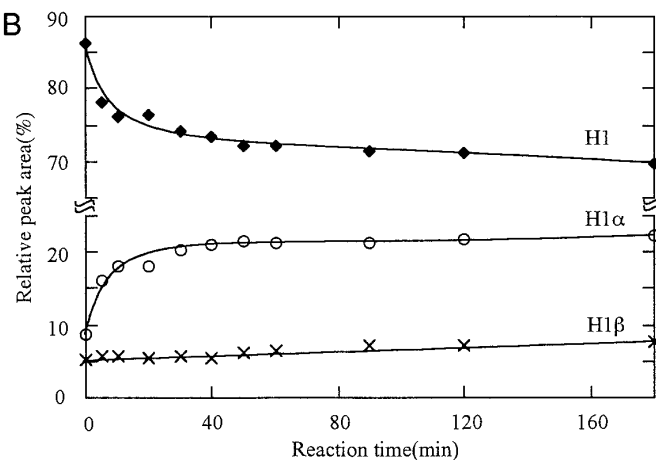
enzyme. In the productive mode, the $(\text{GlcNAc})_3$ moiety of the substrate binds in sites B–D and 4-methylumbelliferyl interacts at site E, although in a different way from a natural substrate GlcNAc group.

As mentioned earlier, we have also proposed that barley chitinase is the archetype of a superfamily of glycohydrolases. The structural similarity among them is likely to give rise to functional similarities as well. Anomeric forms of the products from *Streptomyces* sp. N174 chitosanase and phage T4 lysozyme have been reported to be the α -form (16, 17), and the product from goose egg white lysozyme was also the α -form (Kuroki *et al.*, personal communication). All of these are inverting enzymes, and the barley chitinase investigated in this study was expected to be an inverting one. The anomeric form of the products from chitinase was the α -form, and the result was consistent with anticipation from the structural study.

The results of the pH analysis of chitinase also lend support to the hypothesis about the chitinase mechanism. Figure 1b shows enzyme activity requires the unprotonated form of a group with a $pK_a \sim 3.9$. This is probably Glu 89 acting as a base. Catalysis is independent of pH until values of about 6.5. Activity is then lost as an acid is deprotonated. This is presumably Glu 67, manifesting a pK_a of ~ 6.8 . Although this is high for a carboxylic acid, it is similar to the value observed for the homologous Glu residues of lysozyme. For example the pK_a for Glu 35 of hen egg white lysozyme is 6.7 (18). It may be that binding a substrate polymer dehydrates the active site and dramatically raises the pK_a of this group, which is otherwise exposed to solvent.

The poly(GlcNAc) dissociation constants we measured show the intuitively expected results. A decrease

FIG. 4. (A) ^1H NMR spectrum of chitinase hydrolysis of $(\text{GlcNAc})_6$. Signals at 5.14 and 4.64 ppm are from the anomeric proton of the reducing end of GlcNAc in the α -form and the β -form, respectively. (B) Time course of relative peak areas of individual signals from A. H 1α increased rapidly through the early part of the experiment, while H 1β remained relatively constant.

A**B**

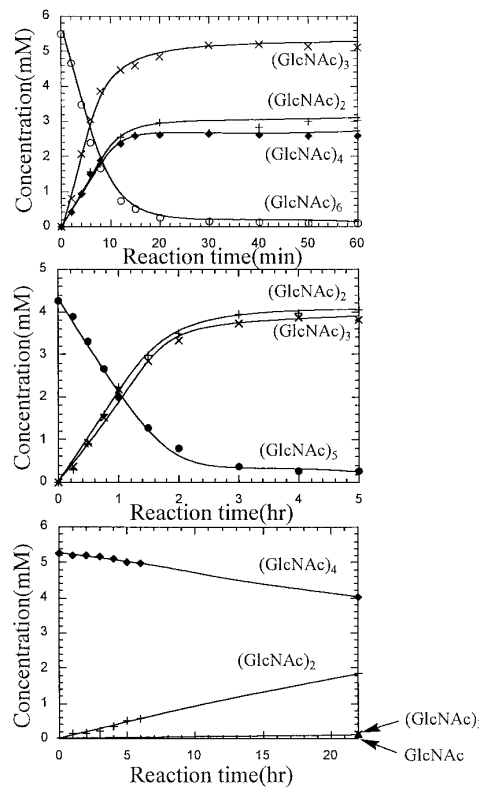


FIG. 5. Time course of (GlcNAc) oligosaccharide degradation catalyzed by chitinase. (Top) (GlcNAc)₆ hydrolysis produced (GlcNAc)₃ as well as (GlcNAc)₄ and (GlcNAc)₂. (Center) (GlcNAc)₅ hydrolysis produced (GlcNAc)₃ and (GlcNAc)₂. (Bottom) (GlcNAc)₄ hydrolysis produced only (GlcNAc)₂.

in K_d , or an increase in K_a , is seen with increasing length of (GlcNAc) polymer. As indicated in Fig. 7, specific contacts for the hydrolyzable substrate are made with the enzyme at sites B–D. These are modeled on the crystallographically observed binding of substrates to lysozymes (11). No crystallographic observations have been made for substrates binding at sites E, F, or higher in lysozyme, suggesting that binding at those aglycone sites is relatively weak. Measurements have been made for the free energy of binding substrates to hen egg white lysozyme (19). These suggest the strongest interactions are made at site C, followed by B at about half the strength, and then A, E, and F at about one-quarter strength. It was observed that interactions at D were unfavorable, consistent with the widely held idea that the substrate at D is distorted into a half-chair configuration to mimic the transition state of the hydrolytic reaction (20), although this interpretation has been questioned based on quantum mechanical and other energy calculations (21).

The poly(GlcNAc) cleavage by barley chitinase presents a picture which is complementary to, but different from, that of lysozyme. We have shown that barley

chitinase cleaves purified (GlcNAc)₆ into several patterns. The main one is cleavage into trimers, (GlcNAc)₃, although cleavage into tetramers and dimers is also common. Recalling that the cleavage point is defined to be between sites D and E, the cleavage patterns suggest that substrate binding across the catalytic site may be more nearly symmetrical than for hen lysozyme. That is, the strength of binding at sites E and F may be relatively greater than that for lysozyme, although it is likely that sugar binding to site D is still not favorable. Short oligomers, dimers and trimers, do not accumulate enough interactions on either side of the D site to bind well. That is, the enthalpic contributions made by hydrogen bonding and Van der Waals interactions over a short span do not compensate for the entropic costs of freezing the saccharide onto the enzyme surface. A polysaccharide can accumulate enough favorable interactions to assure binding by

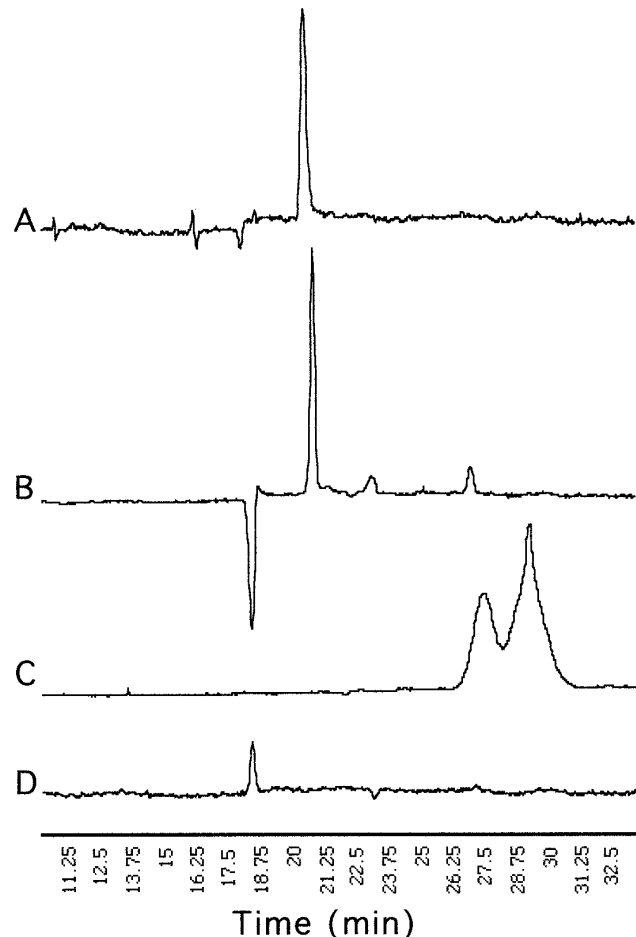


FIG. 6. Capillary electrophoresis separation of (GlcNAc)₃UMB hydrolysis by chitinase. (A) (GlcNAc)₃UMB after 0 h. (B) (GlcNAc)₃UMB after 15 h. (C) (GlcNAc)₂ (27.5 min retention time) and (GlcNAc)₃ (29 min retention time). (D) 4-Methylumbelliflone (18.5 min retention time).

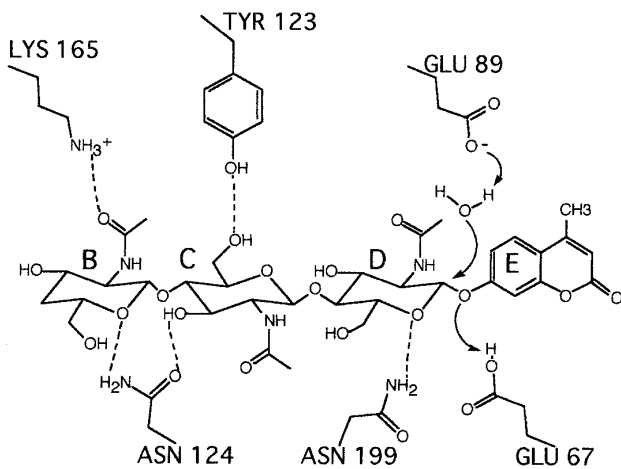


FIG. 7. Schematic binding of the 4-methylumbelliferyl β -N,N,N'-triacetylchitotriose substrate to the active site of barley chitinase. The binding of polysaccharides to the enzyme is based on the model of Hart *et al.* (1995). Glu 67 is the acid which protonates the leaving group, 4-methyl umbelliferone in this case. Glu 89 acts as a base to activate a water molecule attacking the α -side of sugar D in the inverting mechanism.

spanning the catalytic site, binding at A–F. Once hydrolysis has occurred, the two separate oligosaccharides lack the interaction strength to remain firmly bound, and they diffuse away; the aglycone product in sites E and F probably leaves first, while the saccharide binding at stronger sites (C and B) is probably retained longer. The requirement to bind lengthy substrates is consistent with the biological function of the enzyme, which is to hydrolyze a solid chitin matrix on fungal invaders, thereby weakening their walls. There is no selective advantage in binding short oligosaccharides since they do not benefit the host and such binding would only serve to inhibit the defensive enzyme.

The fluorescent model substrate used in our kinetic studies is a (GlcNAc)₃ saccharide with a 4-methylumbelliferyl group as the aglycone. The substrate binds productively as shown in Fig. 7, with GlcNAc groups in sites B–D, and the methylumbelliferyl group at site E. Hydrolysis releases the methylumbelliferyl group, which is measured by its fluorescence. The main product from hydrolysis of (GlcNAc)₃UMB, however, is the result of binding in another conformation, over sites C–F. Consistent with our cleavage patterns, and those of yam chitinase (13), (GlcNAc)₂ and (GlcNAc) umbelliferone are the major hydrolysis products (Fig. 6), which is unproductive for this assay. The productive hydrolysis, however, does show a linear response with time, and its convenience makes it a useful tool for future work characterizing wild-type and mutant chitinases of this class.

The K_m for the (GlcNAc)₃UMB substrate is 33 μM , nearly identical to the values reported for yam chi-

tinase against poly(GlcNAc) substrates (13). The catalytic rate, on the other hand, is 0.3/min, perhaps 50 to 100 times slower than that for the yam enzyme acting on poly(GlcNAc) or for lysozyme acting against natural substrates (22). This can be accounted for by the fact that we are measuring possibly only 1% of the actual hydrolysis taking place. It is the convenience of this substrate, however, that makes it a useful tool for future analysis of wild-type and mutant chitinases.

An interesting observation is that with (GlcNAc)₄, as well as with (GlcNAc)₃UMB, K_m is about $\frac{1}{2}$ to $\frac{1}{3}$ K_d for the ligand. For a simple Michaelis–Menton kinetic model, K_d must always be smaller than K_m , indicating this is an inappropriate model for chitinase.

If the reaction is treated as ordered Bi–Bi, with (GlcNAc)₄ and H₂O as the substrates and (GlcNAc)₂ and (GlcNAc)₂ as the products, experimental parameters can be redefined. Using Cleland nomenclature (23) and the King–Altman method for analyzing steady-state models (24), an equation for initial velocity can be constructed in which

$$K_m = k_2 k_3 k_4 / k_1 k_2 (k_3 + k_4)$$

and

$$K_d = K_{-1} / k_1,$$

where the rate constants are those indicated in Fig. 8. Taking the ratio of these yields

$$K_m / K_d = k_3 k_4 / k_{-1} (k_3 + k_4),$$

where k_{-1} is the first-order dissociation rate of (GlcNAc)₄ and k_3 and k_4 are the dissociation rates of the two (GlcNAc)₂. Without being specific about the numerical values of each constant, it is clear that in the limit they all become equal, the ratio becomes $\frac{1}{2}$, which is very close to the ratio we observe. That is,

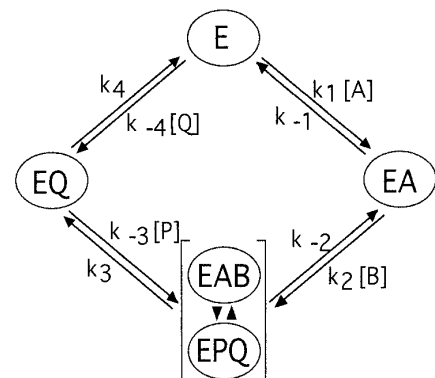


FIG. 8. Kinetic model of chitinase hydrolysis. The reaction is treated as Bi–Bi, with (GlcNAc)₄ and H₂O as the substrates and (GlcNAc)₂ and (GlcNAc)₂ as the products.

we predict that the dissociation rates for the cleaved products of chitinase hydrolysis are about equal to that of the tetrasaccharide substrate. The binding strength of the the tetrasaccharide substrate is not the sum of the two products because it is likely distorted as it spans the catalytic site.

This hypothesis is also consistent with the work of Albery and Knowles (25), who postulate that the evolutionary improvement in the catalytic efficiency of enzymes, compared with simple organic molecules, tends toward "uniform binding." That is, the catalytic efficiency is optimized when differences in free energy of the external states become equal to the differences in the bound states. This tends to equilibrate the free energy differences of all bound species and the first-order rate constants connecting the various steps.

Because of their role as plant defense proteins, chitinases have been the focus of intensifying study in recent years. The kinetic results reported here support the mechanistic hypothesis presented from crystallographic work. They also lay the foundation for further mechanistic analysis of the enzyme by establishing kinetic parameters for the wild-type enzyme using an easily controlled artificial substrate system. Information gained about the mechanisms and characteristics of chitinases has important implications for plant engineering.

ACKNOWLEDGMENTS

We thank Dr. Lawrence Poulsen for helpful discussions about the chitinase kinetics, as well as Dr. Klaus Linse for his help with capillary electrophoresis.

REFERENCES

1. Roberts, W. K., and Selitrennikoff, C. P. (1988) *J. Gen. Microbiol.* **134**, 169–176.
2. Jach, G., Gornhardt, B., Mundy, J., Logemann, J., Pinsdorf, E., Leah, R., Schell, J., and Maas, C. (1995) *Plant J.* **8**, 97–109.
3. Heitz, T., Segond, S., Kauffmann, S., Geoffroy, P., Prasad, V., Brunner, F., Fritig, B., and Legrand, M. (1994) *Mol. Gen. Genet.* **245**, 246–254.
4. Leah, R., Tommerup, H., Svendsen, I., and Mundy, J. (1991) *J. Biol. Chem.* **266**, 1564–1573.
5. Mauch, F., Mauch-Mani, B., and Boller, T. (1988) *Plant Physiol.* **88**, 936–942.
6. Sinshi, H., Neuhaus, J. M., Ryals, J., and Meins, F. (1990) *Plant Mol. Biol.* **14**, 357–368.
7. Collinge, D. B., Kragh, K. M., Mikkelsen, J. D., Nielsen, K. K., Rasmussen, U., and Vad, K. (1995) *Plant J.* **3**, 31–40.
8. Hart, P. J., Pfluger, H. D., Monzingo, A. F., Hollis, T., and Robertus, J. D. (1995) *J. Mol. Biol.* **248**, 402–413.
9. Hart, P. J., Monzingo, A. F., Ready, M. P., Ernst, S. R., and Robertus, J. D. (1993) *J. Mol. Biol.* **229**, 189–193.
10. Robertus, J. D., Hart, P. J., Monzingo, A. F., Marcotte, E., and Hollis, T. (1995) *Can. J. Bot.* **73**(Suppl. 1).
11. Monzingo, A. F., Marcotte, E. M., Hart, P. J., and Robertus, J. D. (1996) *Nature Struct. Bio.* **3**, 133–140.
12. Henrissat, B., and Bairoch, A. (1993) *Biochem. J.* **293**, 781–788.
13. Koga, D., Tsukamoto, T., Sueshige, N., Utsumi, T., and Ide, A. (1989) *Biol. Chem.* **53**, 3121–3126.
14. Dygart, S., Li, H., Florida, D., and Thoma, J. (1965) *Anal. Biochem.* **13**, 367–374.
15. Bruch, R. C., Bruch, M. D., Noggle, J. H., and White, H. B. (1984) *Biochem. Biophys. Res. Commun.* **123**, 555–561.
16. Wang, Q., Graham, R. W., Trimbur, D., Warren, R. A. J., and Withers, S. G. (1994) *J. Am. Chem. Soc.* **116**, 11594–11595.
17. Fukamizo, T., Honda, Y., Goto, S., Boucher, I., and Brzezinski, R. (1995) *Biochem. J.* **311**, 377–383.
18. Banerjee, S. K., Kregar, I., Turk, V., and Rupley, J. A. (1973) *J. Biol. Chem.* **248**, 4786–4792.
19. Chipman, D. M., and Sharon, N. (1969) *Science* **165**, 454–465.
20. Phillips, D. C. (1966) *Sci. Am.* **215**, 78–90.
21. Warshel, A., and Levitt, M. (1976) *J. Mol. Biol.* **103**, 227–249.
22. Imoto, T., Johnson, L. N., North, A. C., Phillips, D. C., and Rupley, J. A. (1972) in *The Enzymes* (Boyer, P. D., Ed.), Vol. 7, 3rd ed., pp. 665–868, Academic Press, New York.
23. Cleland, W. W., (1963) *Biochem. Biophys. Acta* **67**, 104, 173, 188.
24. Segel, I. H. (1975) *Enzyme Kinetics: Behavior and Analysis of Rapid Equilibrium and Steady-State Enzyme Systems*, pp. 506–846, Wiley, New York.
25. Albery, J. W., and Knowles, J. R. (1976) *Biochemistry* **15**, 5631–5640.